https://africanjournalofbiomedicalresearch.com/index.php/AJBR
Afr. J. Biomed. Res. Vol. 27(6s) (December 2024); 586-602
Research Article

Synthesis Of New Bromo Oxazepine Compounds, Biological Evaluation, Molecular Docking Studies, And Simulation Methodology For Anti-Skin Cancer.

B. Brindha[1*], Dr.R. Girija[2], Dr.S. Aruna[3]

[1*,2,3]Department of Chemistry, Queen Mary's College, Bioinformatics Infrastructure Facility Centre, Chennai-600 004. Tamil Nadu.

Abstract:
Heterocyclic compounds are of particular interest, especially in the area of medical chemistry. The bulk of contemporary drugs do, in fact, include a heterocyclic ring. The seven-atom unsaturated heterocycles known as azepines have one spot where a nitrogen atom takes the place of a carbon atom. In a single pot, it is subjected to cyclization and has a fresh 2-aminophenol substituted for the aromatic ring. A possible skin cancer treatment drug (2VCI), 4,5-diaryl isoxazole Hsp90 Chaperone inhibitors, are tested insilico docking studies against bromooxazepine derivatives.

Keywords: Heterocyclic compounds, azepine, bromooxazepine, molecular docking studies

Received: 01/12/2024 Accepted: 10/12/2024

DOI: https://doi.org/10.53555/AJBR.v27i6S.7214

1.Introduction:

A unique class of chemicals known as heterocyclic compounds has been linked to both natural and therapeutic benefits [1, 2]. Chalcone, a derivative of 1,3-diphenyl-2-propen-1-one, has a preferred structure with two aromatic rings connected by an unsaturated, three-carbon carbonyl system. Chalcones are an easily cyclized family of flavonoids that has a wide range of structural variations [3]. An amphoteric chemical called 2-aminophenol acts as a reducing agent. It serves as a useful reagent in the synthesis of heterocyclic compounds [4]. Oxazepine, a heterocyclic substance, has one oxygen atom, one nitrogen atom, and five carbon atoms. Oxazepine derivatives are one type of heterogeneous nitrogen-containing chemical compound that has several medicinal applications [5,6]. The relevance of bromosubstituted oxazepine derivatives is highlighted. The development of novel methodologies based on a multi-component strategy has become an increasingly active area of study in order to generate physiologically active polysubstituted oxygen structures for drug discovery programmes such as bromooxazepine derivatives. Molecular chaperones play a significant role in maintaining the stability, function, and proper folding of various proteins within the cellular environment [7,8]. Among them, Hsp90 is crucial for stabilizing and transporting tyrosine and serine/threonine kinases, which become active when the cell experiences genotoxic stress, and are essential for the survival of cancer cells. In light of this, several Hsp90 inhibitors are currently undergoing phase I/II clinical trials, alongside ionizing radiation (IR) or chemotherapeutic agents, with the aim of evaluating their potential in combating cancer [9-11]. To assess the efficacy of these compounds in inhibiting skin cancer development, both in vitro and in silico investigations were conducted.

2.Materials and methods

2.1 Synthesis of Tetrabromochalcone:

Several heterocyclic compounds, including pyrimidines [12], thiazines [13], flavones [14], aziridine aziridine[15], and benzofurans [16], have been synthesised using bromochalcones as potential intermediates [17]. The Scheme comprises two steps that make up the overall

schematic representation, detailing the synthesis routes. Chalcones (1) were prepared using a water/ethanol solution as the reaction medium. The synthesis involved the combination of Benzaldehyde with acetone, followed by the addition of sodium hydroxide and stirring the mixture for one hour. This process resulted in the formation of Chalcones. On the other hand, Bromochalcone (2) was obtained through a different procedure. Chalcone was subjected to a reaction with liquid Bromine in a chloroform medium. The reaction took place in a chilled ice bath and was stirred for two hours, with the addition of glacial acetic acid.

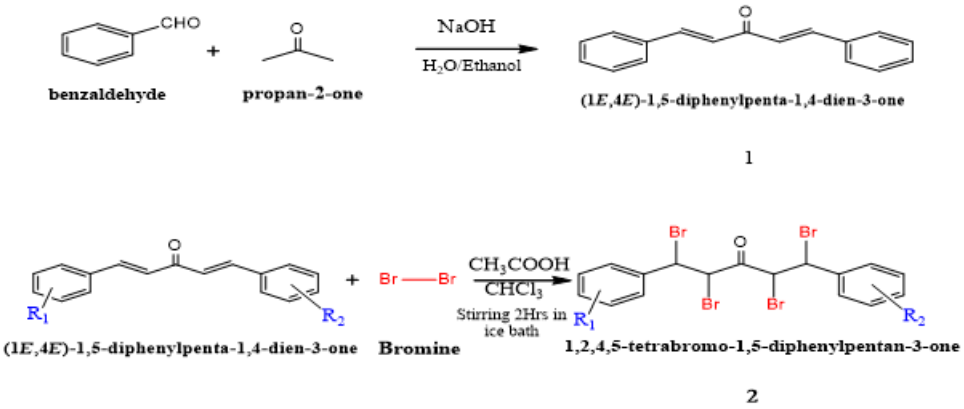

Figure 1: Schematic diagram

3 Experimental Section:

3.1 General Methods:

Thin-layer chromatography (TLC) was utilized to monitor all reactions under standard conditions, employing Merck silica gel 60 F254 precoated plates (0.25 mm). Column chromatography was employed for purification on silica gel. The chemical yields were determined for pure, separated compounds. The 1H and 13C NMR spectra were recorded in a CDCl3 solution, and the spectral data were expressed in ppm relative to the internal standard tetramethylsilane (TMS). The 13C NMR spectra were recorded with perfect proton decoupling. High-resolution mass spectra were obtained using quadrupole electrospray ionization (ESI). Melting points were determined using a melting point instrument. Table 1 displays the observed yields (85-92%) of compounds (1a-1j).

3.2 Procedure for the synthesis of 3-bromo-4-(1, 2-dibromo-2-phenylethyl)-2-phenyl-2, 3-dihydrobenzo[*b*] [1,4]oxazepine derivatives:

To synthesize the bromo oxazepine derivatives, 2-aminophenol and bromo chalcone compounds were mixed with sodium hydroxide in an ethanol medium. The reaction mixture was agitated for another 3-4 hours while being monitored by TLC. Ice-cold water was used to cleanse the mixed organic layers. A silica-gel column was used for purification, and the sample was eluted using CHCl3/hexane. All of the synthesised compounds were analysed and characterised using mass, IR, 1H, and NMR data.

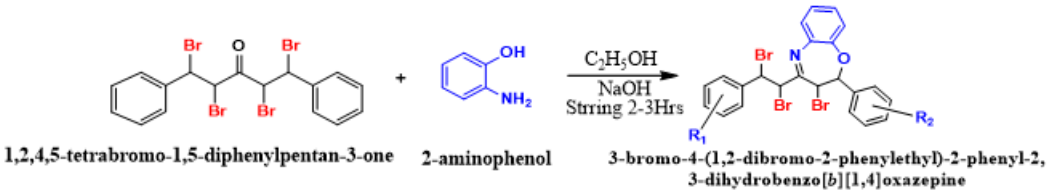

Figure 2: Schematic diagram

R - a R_1&R_2- H, b R_1&R_2- 3,4 dihydroxy c R_1&R_2- 4-Hydroxy, d R_1&R_2- 2-nitro-4-bromo, e R_1&R_2- 4-methoxy, f R_1&R_2-3,4,5-trimethoxy, g R_1&R_2- 4-nitro, h R_1&R_2-2-chloro-4-methyl, i R_1&R_2- 2,3-dimethyl, j R_1&R_2- 2,6-dichloro -4-methyl.

Table 1: Physical Data of Compounds (1a-1j)

Compound	Compound Name	Reaction Time (Hours)	Yield (%)	Melting point^{0}C
3A	3-bromo-4-(1,2-dibromo-2-phenylethyl)-2-phenyl-2,3-dihydrobenzo[*b*] [1,4] oxazepine	2 Hrs	92%	113° C -115° C
3B	4-(3-bromo-4-(1,2-dibromo-2-(3,4-dihydroxyphenyl) ethyl)-2,3-dihydrobenzo[*b*] [1,4] oxazepin-2-yl) benzene-1,2-diol	3 Hrs	91%	162° C -164° C
3C	4-(3-bromo-4-(1,2-dibromo-2-(4-hydroxyphenyl) ethyl)-2,3-dihydrobenzo[*b*] [1,4] oxazepin-2-yl) phenol	3 Hrs	89%	117° C -119° C
3D	3-bromo-2-(4-bromo-2-nitrophenyl)-4-(1,2-dibromo-2-(4-bromo-2-nitrophenyl) ethyl)-2,3-dihydrobenzo[*b*] [1,4] oxazepine	3Hrs	90%	186° C -189° C
3E	3-bromo-4-(1,2-dibromo-2-(4-methoxyphenyl) ethyl)-2-(4-methoxyphenyl)-2,3-dihydrobenzo[*b*] [1,4] oxazepine	2Hrs	90%	158° C -159° C
3F	3-bromo-4-(1,2-dibromo-2-(3,4,5-trimethoxyphenyl) ethyl)-2-(3,4,5-trimethoxyphenyl)-2,3-dihydrobenzo[b] [1,4] oxazepine	4 Hrs	91%	168° C -170° C
3G	3-bromo-4-(1,2-dibromo-2-(4-nitrophenyl) ethyl)-2-(4-nitrophenyl)-2,3-dihydrobenzo[b] [1,4] oxazepine	2 Hrs	90%	156° C -157° C
3H	3-bromo-2-(2-chloro-4-methylphenyl)-4-(1,2-dibromo-2-(2-chloro-4-methylphenyl) ethyl)-2,3-dihydrobenzo[b] [1,4] oxazepine	3Hrs	91%	127° C -129° C
3I	3-bromo-4-(1,2-dibromo-2-(2,3-dimethylphenyl) ethyl)-2-(2,3-dimethylphenyl)-2,3-dihydrobenzo[b] [1,4] oxazepine	3Hrs	88%	158° C -160° C
3J	3-bromo-4-(1,2-dibromo-2-(2,6-dichloro -4-methylphenyl) ethyl)-2-(2,6-dichloro-4-methylphenyl)-2,3-dihydrobenzo[b] [1,4] oxazepine	3Hrs	87%	181° C -182° C

Table 2: Characterization of 3-bromo-4-(1, 2-dibromo-2-phenylethyl)-2-phenyl-2, 3-dihydrobenzo[*b*] [1, 4] oxazepine(3A)

^{1}H NMR	δ 7.610-6.697(multiplet-aromaticprotons) δ 6.657 (d-, methylene proton) δ 5.532, 4.202,4.188(d, bromides protons)
^{13}C NMR	δ 67.98(Aliphatic-CO carbon, S) [77.35(1C, S),77.04(1C S),76.72(1C, S) (methylbromide)],139.21,134.61,133.97,131.07,130.90,130.54,130.45,130.29,129.03,128.99,128.96, 123.85,128.74,128.67,121.06 (Aromatic carbon, S) 143.38 (Ar-CHBr, s), 145.93 (Ar-CO carbon, s), 146.52 (Aliphatic-CN carbon, s),
Mass (m/z)	564.88
IR	3055.65 (Aromatic C-H), 1706.9 (C=O), 692.32, 553.47, 515.86(C-Br), 1202.9 (C=N)

Table 3: Characterization of 4-(3-bromo-4-(1,2-dibromo-2-(3,4- dihydroxyphenyl) ethyl)2, dihydrobenzo[*b*][1,4]oxazepin-2-yl) benzene-1,2-diol(3B)

^{1}H NMR	δ 7.624- 6.531(multiplet-aromatic protons) δ 6.048 (d-, methylene proton) δ 5.491,4.658,4.624(d, bromides protons)
^{13}C NMR	δ 68.35(Aliphatic-CO carbon, S) [77.56(1C, S),77.25(1C S),76.54(1C, S) (methyl bromide)],131.52,130.94,130.15,130.05,129.45,128.95,128.89,128.65,128.57,123 .51,121.45,115.7 (Aromatic carbon, S) 144.24 (Ar-CHBr, s), 146.33 (Ar-CO carbon, s), 147.12 (Aliphatic-CN carbon, s), 140.52,140.42,139.27,139.17(Ar C-OH carbon, s)
Mass (m/z)	628.11
IR	3102.22 (Aromatic C-H), 1741.12 (C=O), 695.12, 555.32, 517.96(C-Br), 1205.81(C=N)

Table 4: Characterization of 4-(3-bromo-4-(1,2-dibromo-2-(4-hydroxyphenyl)ethyl)2,3dihydrobenzo[*b*][1,4]oxazepin-2-yl)phenol(3C)

^{1}H NMR	δ 7.653-6.596(multiplet-aromaticprotons) δ 6.612 (d-, methylene proton) δ 5.432, 4.202,4.188(d, bromides protons)
^{13}C NMR	δ 68.98(Aliphatic-CO carbon, S) [77.45(1C, S),77.14(1C S),76.12(1C, S) (methyl bromide)],131.52,130.94,130.15,130.05,129.45(2C,d),128.89(2C,d),123.51,121.4 5, 115.7(2C d) (Aromatic carbon, S) 144.24 (Ar-CHBr, s), 146.78 (Ar-CO carbon, s), 147.12 (Aliphatic-CN carbon, s), 140.52,140.42,139.27,139.17(Ar C-OH carbon, s)
Mass (m/z)	596.112
IR	3072.54 (Aromatic C-H), 1712.81 (C=O), 696.41, 556.47, 518.12(C-Br), 1208.5 (C=N) cm-1.

Table 5: Characterization of 3-bromo-2-(4-bromo-2-nitrophenyl)-4-(1,2-dibromo-2-(4-bromo-2-nitrophenyl)ethyl)-2,3-dihydrobenzo[*b*][1,4]oxazepine(3D)

^{1}H NMR	δ 7.670-6.679(multiplet-aromaticprotons) δ 6.123 (d-, methylene proton) δ 5.151, 4.923,4.711(d, bromides protons)
^{13}C NMR	δ 67.98(Aliphatic-CO carbon, S) [77.35(1C, S),77.04(1C S),76.72(1C, S) (methyl bromide)],133.97,131.07,130.90,130.54,130.45,130.29,129.03,128.99,128.96, 123.85,128.74, (Aromatic carbon, S) 146.38 (Ar-CHBr, s), 145.93 (Ar-CO carbon, s), 148.13 (Aliphatic-CN carbon, s), 121.06,121.43((Ar-CBr).142.12,142.87(Ar-C-NO_2)
Mass (m/z)	811.901
IR	3164.15 (Aromatic C-H), 1716.5 (C=O), 694.54, 554.37, 520.75(C-Br), 1212.8 (C=N) cm-1

Table 6: Characterization of 3-bromo-4-(1,2-dibromo-2-(4-methoxyphenyl)ethyl)-2-(4-methoxyphenyl)-2,3-dihydrobenzo[*b*][1,4]oxazepineI(3E)

^{1}H NMR	δ 7.686-6.668(multiplet-aromaticprotons) δ 6.257 (d-, methylene proton) δ 5.253, 4.315,4.214(d, bromides protons) δ 3.713(s, methoxy proton)
^{13}C NMR	δ 68.98(Aliphatic-CO carbon, S) [77.31(1C, S),77.12(1C S),76.72(1C, S) (methyl bromide)],140.72,140.32,139.17,139.11,131.52,130.57,130.25,130.14,129.35,128.89,123.51,121.45, 115.7(2C d) (Aromatic carbon, S) 144.24 (Ar-CHBr, s), 146.14 (Ar-CO carbon, s), 147.12 (Aliphatic-CN carbon, s), 151.16(2C Ar-methoxy,s),51.12(2C methoxy carbon,s)
Mass (m/z)	624.166
IR	3066.12 (Aromatic C-H), 1718.2(C=O), 695.34, 555.47, 522.7(C-Br), 1214.32(C=N), 2906 (C-OCH_3) cm-1

Table 7: Characterization of 3-bromo-4-(1,2-dibromo-2-(3,4,5-trimethoxyphenyl)ethyl)-2-(3,4,5-trimethoxyphenyl)-2,3-dihydrobenzo[b] [1,4] oxazepine(3F)

^{1}H NMR	δ 7.652-6.679(multiplet-aromaticprotons) δ 6.657 (d-, methylene proton) δ 5.532, 4.202,4.188(d, bromides protons)
^{13}C NMR	δ 68.45(Aliphatic-CO carbon, S) [77.89(1C, S),77.57(1C S),76.47(1C, S) (methyl bromide)],139.21,134.61,133.97,131.07,130.45,130.29,129.03,128.99,128.96,123.85,128.74,128.67,121.06,114.51 (Aromatic carbon, S) 143.38 (Ar-CHBr, s), 145.93 (Ar-CO carbon, s), 146.52 (Aliphatic-CN carbon, s), 154.16,139.23(2C,1C Ar-methoxy,s), 52.64(3C methoxy carbon,s)
Mass (m/z)	744.27
IR	3168.15 (Aromatic C-H), 1720.9 (C=O), 697.12, 556.52, 523.16(C-Br), 1215.45 (C=N)

Table 8: Characterization of 3-bromo-4-(1,2-dibromo-2-(4-nitrophenyl)ethyl)-2-(4-nitrophenyl)-2,3-dihydrobenzo[b][1,4]oxazepine(3G)

^{1}H NMR	δ 7.674-6.666(multiplet-aromaticprotons) δ 6.072 (d-, methylene proton) δ 5.124, 4.519,4.437(d, bromides protons)
^{13}C NMR	δ 65.18(Aliphatic-CO carbon, S) [77.75(1C, S),77.12(1C S),76.82(1C, S) (methyl bromide)],135.21,134.82,133.85,131.17,130.20,130.14,130.11,129.29,129.03,128.45,128.16, 123.85,128.74,128.38,121.16 (Aromatic carbon, S) 143.38 (Ar-CHBr, s), 145.93 (Ar-CO carbon, s), 146.14 (Aliphatic-CN carbon, s), 145.93 (Ar-C-NO_2)
Mass (m/z)	654.108
IR	3067.65 (Aromatic C-H), 1716.51 (C=O), 693.72, 555.68, 517.23(C-Br), 1216.15 (C=N)

Table 9: Characterization of 3-bromo-2-(2-chloro-4-methylphenyl)-4-(1,2-dibromo-2-(2-chloro-4-methylphenyl) ethyl)-2,3-dihydrobenzo[b][1,4]oxazepine(3H)

^{1}H NMR	δ 7.615-6.669(multiplet-aromaticprotons) δ 6.247 (d-, methylene proton) δ 5.532, 4.112,4.012(d, bromides protons) 2.06 (methyl protons).
^{13}C NMR	δ 66.79. (Aliphatic-CO carbon, S) [77.32(1C, S),77.42(1C S),76.14(1C, S) (methyl bromide)],139.21,134.61,133.97,131.07,130.90,130.54,130.45,130.29,129.03,128 .99,128.96, 123.85,128.74,128.67,121.06 (Aromatic carbon, S) 143.38 (Ar-CHBr, s), 21.23(2C Ar-C-Me,s) 146.32 (Ar-CO carbon, s), 146.54 (Aliphatic-CN carbon, s)
Mass (m/z)	661.057
IR	3072.65 (Aromatic C-H), 17.9 (C=O), 664.12, 556.18, 517.36(C-Br), 1214.8 (C=N) 1409.89 (C-CH3) cm-1.

Table 10: Characterization of 3-bromo-4-(1,2-dibromo-2-(2,3-dimethylphenyl) ethyl)-2-(2,3-dimethylphenyl)-2,3-dihydrobenzo[b] [1,4] oxazepine(3I)

^{1}H NMR	δ 7.658-6.695(multiplet-aromaticprotons) δ 6.657 (d-, methylene proton) δ 5.532, 4.202,4.188(d, bromides protons), 2.26 (methyl protons)
^{13}C NMR	δ 67.19(Aliphatic-CO carbon, S) [77.58(1C, S),77.18(1C S),76.52(1C, S) (methyl bromide)],139.67,134.64,133.95,131.17,130.91,130.74,130.45,130.41,129.13,128 .97,128.96, 128.76,128.45, 123.25,121.16 (Aromatic carbon, S) 143.38 (Ar-CHBr, s), 145.93 (Ar-CO carbon, s), 146.57 (Aliphatic-CN carbon, s), 28.23,20.14(2C,2C methyl carbon, s)
Mass (m/z)	620.22
IR	3062.13 (Aromatic C-H), 1712.8 (C=O), 62.32, 555.47, 516.86(C-Br), 1215.72(C=N)

Table 11: Characterization of 3-bromo-4-(1,2-dibromo-2-(2,6-dichloro -4-methylphenyl) ethyl)-2-(2,6-dichloro-4-methylphenyl)-2,3-dihydrobenzo[b] [1,4] oxazepine(3J)

^{1}H NMR	δ 7.610-6.607(multiplet-aromaticprotons) δ 6.542 (d-, methylene proton) δ 5.578, 4.245,4.101(d, bromides protons), 2.56 (methyl protons)
^{13}C NMR	δ 67.42(Aliphatic-CO carbon, S) [77.37(1C, S),77.32(1C S),76.51(1C, S) (methyl bromide)],139.11,134.85,133.67,131.21,130.80,130.55,130.15,130.09,129.13,128 .87,128.54, 128.74,128.41, 123.14,121.12 (Aromatic carbon, S) 143.64 (Ar-CHBr, s), 145.97 (Ar-CO carbon, s), 146.62 (Aliphatic-CN carbon, s), 22.14(methyl C, s),132.7(2C, Ar-C-Cl,s)
Mass (m/z)	729.947
IR	3157.24 (Aromatic C-H), 1727.4 (C=O), 696.32, 562.47, 520.17(C-Br), 1218.5 (C=N)

Figure 3: 1H NMR Spectrum

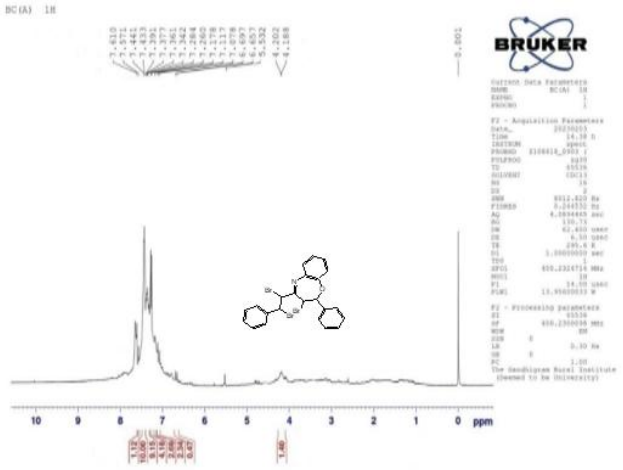

Figure 4: 13C NMR Spectrum

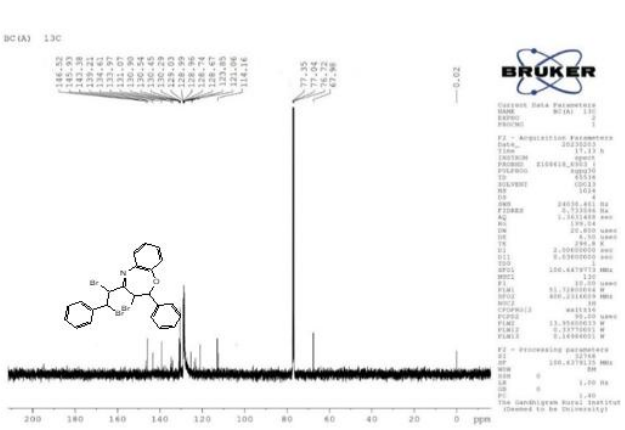

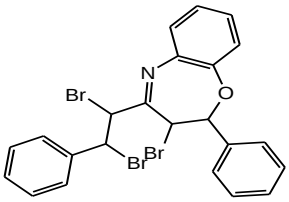

Figure 5: Mass Spectrum

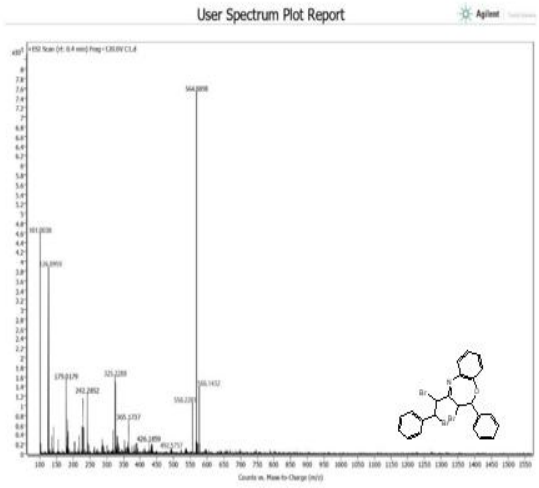

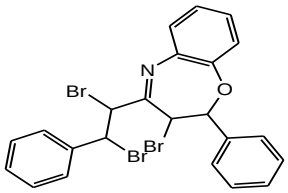

Figure 6: IR Spectrum

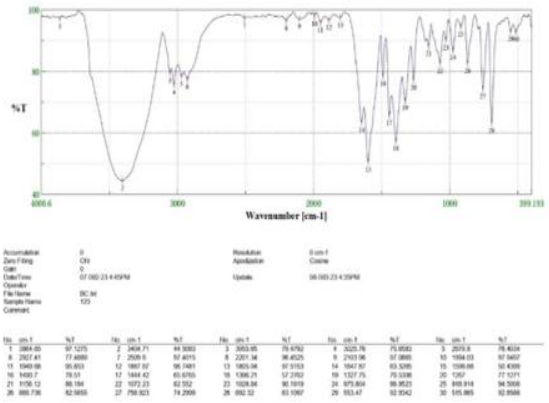

4. Docking Study:

As a result of the completion of the human genome project, a rising number of novel therapeutic targets are becoming available for drug development. [18] The advancement of nuclear magnetic resonance spectroscopy, crystallography, and high-throughput protein purification procedures has also contributed to a better knowledge of the structural characteristics of proteins and protein-ligand complexes. These advancements now allow computational tools to be applied in all stages of drug discovery. [19]

Ligand docking studies were carried out using SCHRODINGER's GLIDE module to investigate the interactions between ten chemicals and proteins. This technique predicted the optimal binding interactions between the ligands and the proteins. Each compound's structure was initially created using CHEMDRAW ULTRA 12.0 and then converted from .sdf to .mae format in MAESTRO 12.1 before ligand preparation. Computational assessment of ADMET properties was performed using Schrodinger Maestro and Schrodinger Qikprop programs, and the results were compared against the Pfizer Rule of 5 and Ghose Filter Rule for Bioavailability standards [20-24].

4.1 Preparation of Ligands:

LigPrep, a valuable application, utilizes energy minimization with OPLS_2005 force field for custom ligand filtering, making it highly useful for subsequent computational research. The 3D structures of the ligands were obtained from the Pubchem database and evaluated using Schrodinger's QikProp module [17] to assess various ADMETox properties, including Rule of Five compliance, oral absorption, CNS penetration, QPPMDCK, etc [25].

Qikprop from Schrodinger Software is a fast, precise, and user-friendly absorption, distribution, metabolism, and excretion prediction application. It forecasts the individual or cumulative pharmaceutically relevant properties of organic substances. This tool assesses compounds based on the Lipinski rule, a set of criteria for active oral drugs. According to these rules, a viable oral drug should meet specific requirements: its molecular weight should fall within the range of 560 to 750 Da, log P should be 5 or lower, the number of H-bond donors should be between 0 and 5, and the number of H-bond acceptors should be between 1 and 7 [26].

Title	Mol MW	donorHB	acceptHB	QPlogPo/w	QPlogS	QPPCaco	QPlogBB	QPPMDCK	QPlogKp	#metab	QPlogKhsa	Human oral absorption	Percent Human Oral Absorption	PSA	Rule Of Five	CNS	#rtvFG
3A	564.113	0	1.75	7.844	-8.674	9506.784	0.732	10000	0.592	6	1.682	1	100	20.818	2	2	4
3B	628.111	4	4.75	4.538	-6.387	118.013	-1.463	364.724	-3.472	8	0.715	1	77.641	107.845	1	-2	4
3C	596.112	2	3.25	6.465	-8.199	889.142	-0.539	2856.531	-1.498	6	1.328	1	91.661	63.554	2	0	4
3D	811.901	0	3.75	7.644	-9.793	412.915	-0.594	7013.232	-2.481	6	1.709	1	92.603	103.705	2	0	4
3E	624.166	0	3.25	7.963	-8.974	9489.113	0.605	10000	0.392	6	1.634	1	100	37.111	2	2	4
3F	744.27	0	6.25	8.146	-8.886	9565.526	0.31	10000	0.282	10	1.507	1	100	62.544	2	1	4
3G	654.108	0	3.75	6.377	-8.578	140.033	-1.426	366.2	-3.298	6	1.524	1	76.779	104.826	2	-2	4
3H	661.057	0	1.75	9.185	-10.696	9505.251	0.946	10000	-0.018	6	2.22	1	100	19.713	2	2	4
3I	620.22	0	1.75	8.852	-10.059	9608.132	0.704	10000	0.053	10	2.233	1	100	20.835	2	2	4
3J	729.947	0	1.75	9.814	-11.426	9582.903	1.139	10000	-0.187	6	2.394	1	100	19.451	2	2	4

Table 12. Qikprop Results of the compound

4.2 Molecular dynamics simulation:

We conducted molecular dynamics simulations on specific docked complexes identified through XP analysis using Desmond, a component of Schrodinger's Biosuite, to investigate their stability [27-29]. These complexes consist of the protein component of the 2VCI (4,5-diarylisooxazole HSP90 chaperone inhibitors) complex with 3-bromo-4-(1,2-dibromo-2-phenylethyl)-2-phenyl-2,3-dihydrobenzo[b] [1,4] oxazepine. The MD simulation was limited to 50 ns and initiated using System Builder, which set up the solvent model, force field, and boundary conditions. [30]

Using the OPLS 2005 force field, we conducted MD simulations on the complexes, filling them with TIP3P water molecules. To satisfy the orthorhombic box boundary conditions, the complexes were centered at a distance of 10 units. The steepest descent technique was employed to minimize the energy of the complex structures to their absolute minimum, serving as Desmond's equilibration procedure. The simulations were run for a duration of up to 100 ns in the NPT ensemble class to simulate complex and realistic conditions.

To assess the ligand's stability within the protein's binding site, we performed simulated event analysis. The behavior and interactions of the ligand within the binding area were evaluated using parameters such as the root-mean-square-distance of the protein-ligand bond, the root-mean-square-free energy, and protein-ligand interactions. [30,31]

4.3 Results:

Protein data Bank (PDB):

The 3D structures of the 4,5 Diaryl Isoxazole Hsp90 Chaperone Inhibitors: Potential Therapeutic Agents for Cancer are available from Protein Data Bank (PDB ID: 2VCI) [32].

Figure 7: 4,5 Diaryl Isoxazole Hsp90 Chaperone Inhibitors (PDB ID: 2VCI)

XP Docking analysis:

The selected drug was docked with the target protein, 4,5-Diaryl Isoxazole Hsp90 Chaperone Inhibitors (2VCI), using XP docking. Additionally, ten oxazepine derivative compounds were subjected to XP docking. The results revealed variations in the dock scores and positions of the top three compounds among the oxazepine derivatives. The top-ranked compound was 4-(3-bromo-4-(1,2-dibromo-2-(4-hydroxyphenyl)ethyl)-2,3-dihydrobenzo[b][1,4]oxazepin-2-ylphenol, which

formed two hydrogen bonds with Leu 48 and Ser 52, and had a dock score of -5.1 kcal/mol. The second-ranked compound was 3-bromo-4-(1,2-dibromo-2-(4-methoxyphenyl)ethyl)-2-(4-methoxyphenyl)-2,3-dihydrobenzo[b][1,4]oxazepine, forming one hydrogen bond with Asn 51, and a dock score of -3.6 kcal/mol. In the third position, 3-bromo-4-(1,2-dibromo-2-phenylethyl)-2-phenyl-2,3-dihydrobenzo[b][1,4]oxazepine, formed one hydrogen bond with Lys 58 (a p-cation), and had a dock score of -3.5 kcal/mol. The standard drug, Binimetinib, interacted with three residues (Lys 58, Gly 07, and Leu 107) forming three hydrogen bonds and had a dock score of -6.0 kcal/mol. Out of the ten oxazepine derivatives, nine compounds showed interactions with the target protein, while one compound showed no interactions

Figure 8: Molecular docking of structure 3C and Standard drug

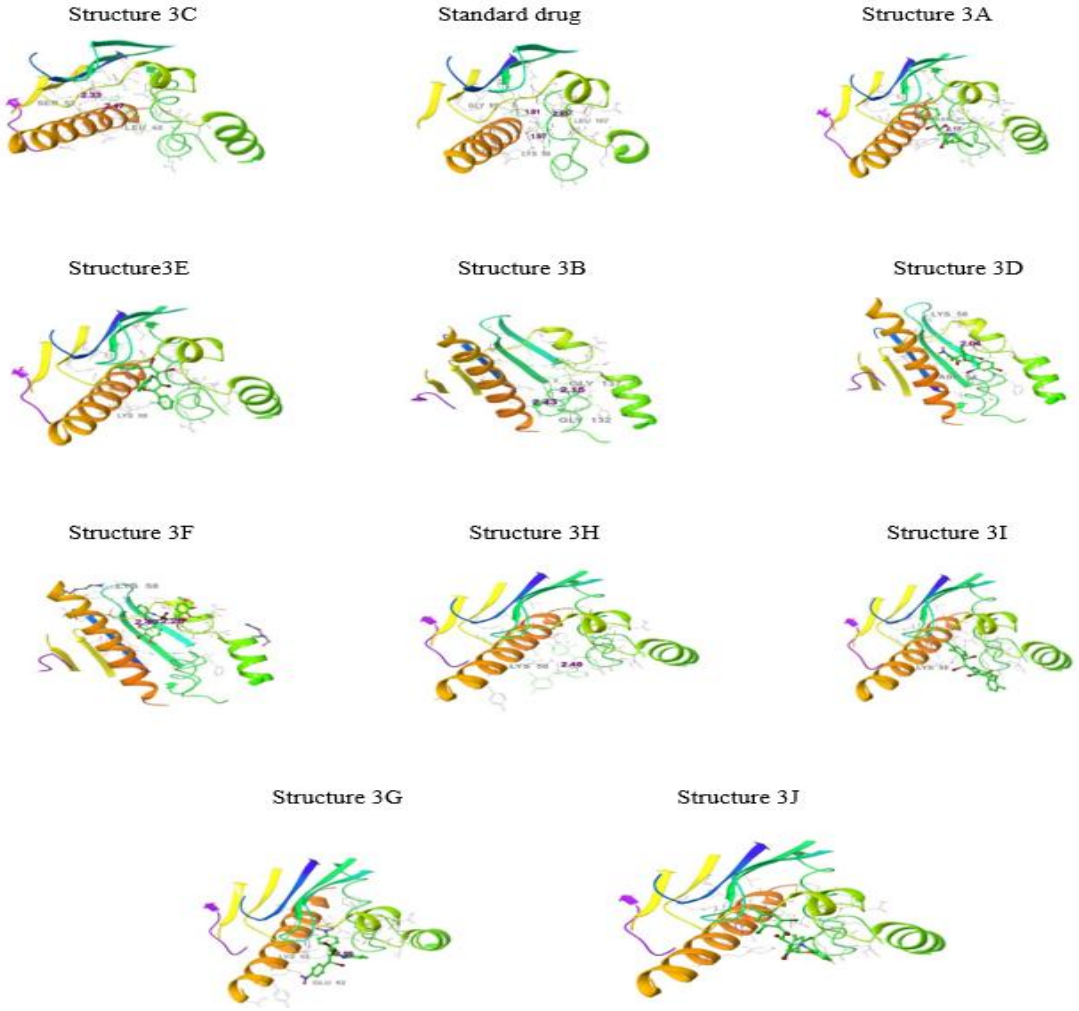

Table 13. XP Docking Results of the compounds

S.No	Compound Name	Dock Score	No of Residues	Interacting residues	Bond Length
1.	Structure 3C	-5.1	2	Leu 48, Ser 52	2.47, 2.33
2.	Structure 3E	-3.6	1	Asn 51	2.17
3.	Structure 3A	-3.5	1	Lys 58 (Pi-cation)	3.47
4.	Structure 3B	-3.3	2	Gly 132, Gly 137	2.43, 2.15
5.	Structure 3D	-3.1	3	Asp 54 (salt bridge), Lys 58(2) (salt bridge)	4.76, 2.04, 3.75
6.	Structure 3F	-2.3	3	Lys 58(3) (salt bridge)	2.26, 2.40, 3.29
7.	Structure 3H	-1.4	1	Lys 58	2.48
8.	Structure 3I	-1.4	1	Lys 58 (pi-cation)	3.39
9.	Structure 3G	-0.7	3	Lys 58 (2) (Pi-cation), Glu 62 (salt bridge)	1.98, 3.64, 4.17
10.	Structure 3J	0.8	-	-	-
	Standard Drug	-6.0	3	Lys 58, Gly 07, Leu 107	1.97, 1.91, 2.43

Binding free energy calculation:

The free energies of target-ligand complexes may be calculated using Table 7. In this case, the bigger the negative number, the stronger the bond. The binding affinity of the Standard medication was discovered to be -37.21. The binding affinity of Structure 3 was greater than that of a conventional medication. Structure 6 in our study has fairly inadequate free energy values when compared to other target-ligand complexes. As a standard, the majority of the compounds have a rather high binding affinity. Structure 5 has the closest free energy value to the reference ligand value.

Table 14: Binding free energy calculations of the compound

S.No	Compound	MMGBSA dG Bind
1.	Structure 3C	-48.4
2.	Structure 3E	-38.12
3.	Structure 3A	-12.29
4.	Structure 3B	-30.91
5.	Structure 3D	-32.14
6.	Structure 3F	-9.42
7.	Structure 3H	-14.52
8.	Structure 3I	-23.77
9.	Structure 3G	-29.15
10.	Structure 3J	-33.23
11.	**Standard Drug**	**-37.21**

Molecular dynamic simulation:

RMSD analysis:

A complex docked structure of the 4,5-Diaryl Isoxazole Hsp90 Chaperone Inhibitors Component with 4-(3-bromo-4-(1,2-dibromo-2-(4-hydroxyphenyl) ethyl) was used to assess stability. It was produced (-2,3 dihydrobenzo[b][1,4] oxazepin-2-yl). The RMSD values illustrate the stability of complex systems when analysed using the RMSD plot. Between 30 to 50 ns, the complex demonstrated stability, with the heavy ligand atoms and the protein's C alpha atoms showing variations within a 3A range. This indicates a strong interaction between the ligand and the protein, making the complex more stable. [33]

Figure 9: RMSD plot of the docked complex structure of 4,5-Diaryl Isoxazole Hsp90 Chaperone with 4-(3-bromo-4-(1,2-dibromo-2-(4-hydroxyphenyl) ethyl)-2,3 dihydrobenzo[*b*] [1,4] oxazepin-2-yl)

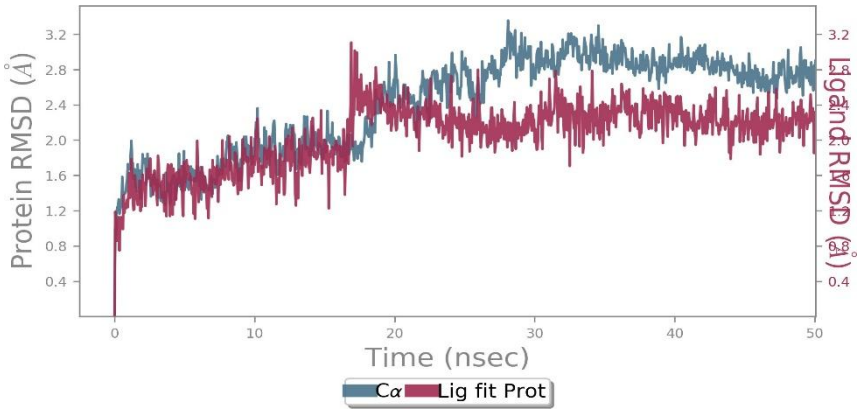

RMSF analysis:

RMSF analysis was used to describe how the protein chain changed throughout the simulation. The residues from the range of 45 to 70 showed a small fluctuation, but the remaining were within the acceptable range. [34]

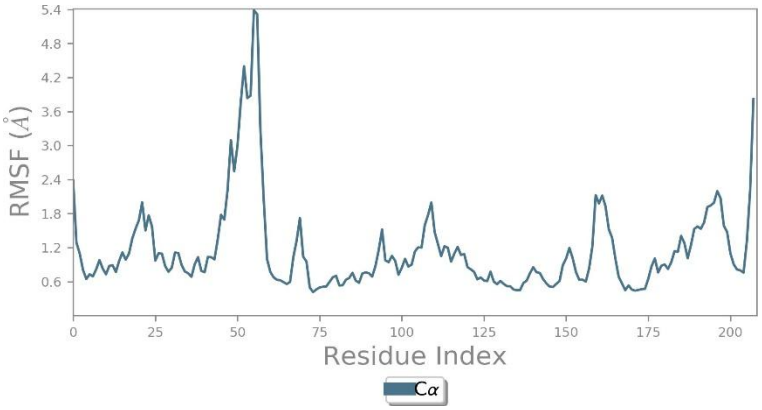

Figure 10: RMSF plot of the docked complex structure of 4,5-Diaryl Isoxazole Hsp90 Chaperone with 4-(3-bromo-4-(1,2-dibromo-2-(4-hydroxyphenyl) ethyl)-2,3 dihydrobenzo[*b*] [1,4] oxazepin-2-yl)

Protein-ligand interactions:

Proteins and their ligands can engage in four distinct types of interactions: hydrogen bonds, hydrophobic bonds, water bridges, and ionic bonds. Among these, hydrogen bonds play a crucial role in pharmaceutical design as they significantly influence drug selectivity, metabolism, and absorption. [35,36]

In the complex structure of 4,5-Diaryl Isoxazole Hsp90 Chaperone Inhibitors with 4-(3-bromo-4-(1,2-dibromo-2-(4-hydroxyphenyl)ethyl)-2,3-dihydrobenzo[b][1,4]oxazepin-2-yl), a prominent hydrogen bond was observed between the ligand and key residues, indicating a strong interaction at the binding site. Hydrogen interactions involved LEU 48, SER 50, ASN 51, SER 52, ASP 93, GLY 97, and THR 184. Additionally, water bridges were formed by GLU 47, ASN 51, ASP 93, and GLY 97, while hydrophobic connections were established by ALA 55, MET 98, LEU 107, PHE 138, and VAL 186 [Refer to Figure 9].

The residues ASN 51, SER 52, ALA 55, ASP 93, GLY 97, etc., maintained the contacts for the longest possible time throughout the simulation, according to the Timeline representation. (Ref. Figure 10)

The 2D picture of the complexed structure demonstrates that the interactions between the residues ASP 93, GLY 97, THR 184, SER 52, and SER 50 were maintained during the simulation period in proportions of 98%, 57%, 39%, 88%, and 64%, respectively. The interaction between 4,5-Diaryl Isoxazole Hsp90 Chaperone Inhibitors and 4-(3-bromo-4-(1,2-dibromo-2-(4-hydroxyphenyl) ethyl)-2,3 dihydrobenzo[*b*][1,4] oxazepin-2-yl) is depicted in Fig. 11 below.

According to the results of the Molecular Dynamics simulation study, the complex formed between 4-(3-bromo-4-(1,2-dibromo-2-(4-hydroxyphenyl)ethyl)-2,3-dihydrobenzo[b][1,4]oxazepin-2-yl) and 4,5-Diaryl Isoxazole Hsp90 Chaperone exhibited stability. Notably, it showed strong interactions with functionally conserved residues Ser 50 and Ser 52, as well as with the interacting residue Leu 48, Ser 52 in the XP analysis. As a result of this simulation investigation, it is suggested that 4-(3-bromo-4-(1,2-dibromo-2-(4-

hydroxyphenyl)ethyl)-2,3-dihydrobenzo[b][1,4]oxazepin-2-yl) may possess potential anticancer effects against 4,5-Diaryl Isoxazole Hsp90 Chaperone.

Figure 11: Graph illustrating the interactions between proteins and ligands in a docked complex structure of 4,5-Diaryl Isoxazole Hsp90 Chaperone with 4-(3-bromo-4-(1,2-dibromo-2-(4-hydroxyphenyl) ethyl)-2,3 dihydrobenzo[*b*] [1,4] oxazepin-2-yl)

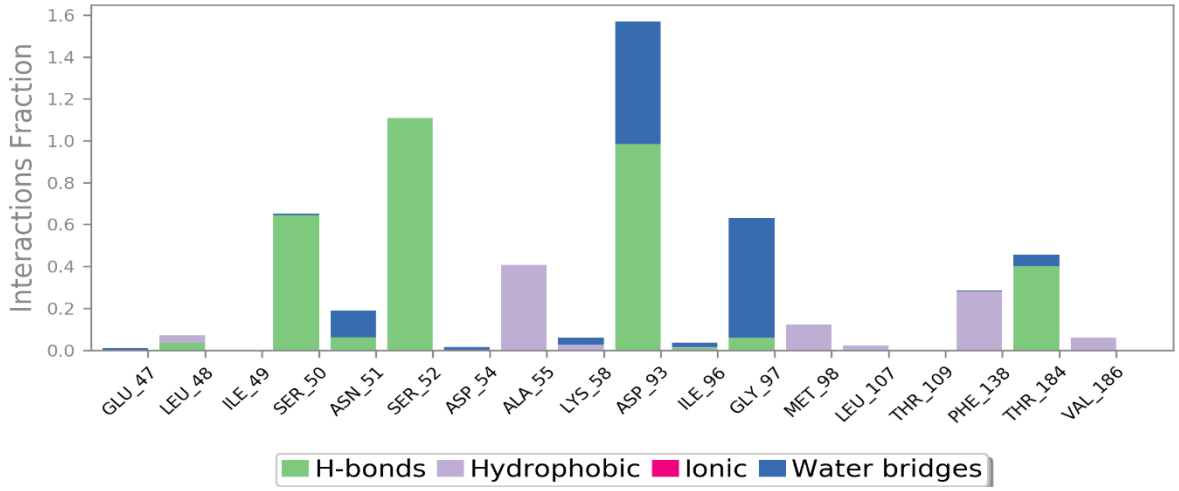

Figure 12: Timeline representation of complex of 4,5-Diaryl Isoxazole Hsp90 Chaperone with 4-(3-bromo-4-(1,2-dibromo-2-(4-hydroxyphenyl) ethyl)-2,3 dihydrobenzo[*b*] [1,4] oxazepin-2-yl)

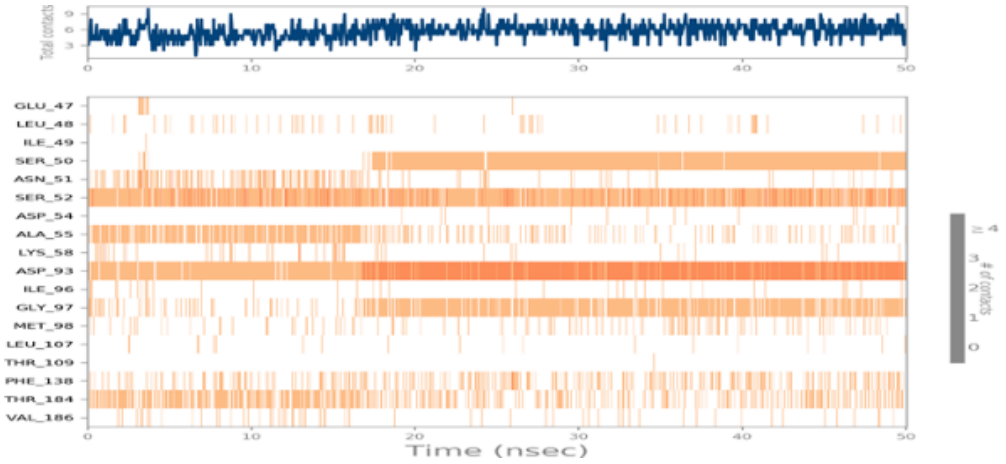

Figure 13: 2D structure of interaction of 4,5-Diaryl Isoxazole Hsp90 Chaperone with 4-(3-bromo-4-(1,2-dibromo-2-(4-hydroxyphenyl) ethyl)-2,3 dihydrobenzo[*b*] [1,4] oxazepin-2-yl)

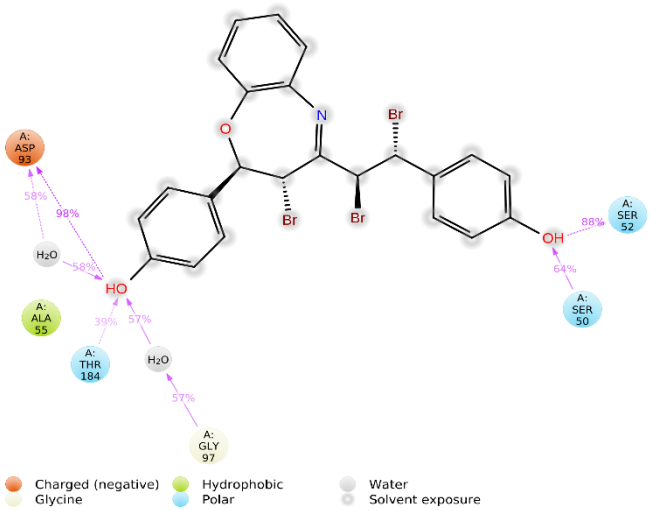

5. In Vitro assay for Anticancer activity: (MTT assay) (Mosmann, 1983):

We obtained the A431 cell line from the Pune-based National Centre for Cell Sciences (NCCS). DMEM was supplemented with 10 percent FBS, 100 U/ml penicillin, and 100 g/ml streptomycin to keep the cells alive and well during culture. This was followed by 37 degrees Celsius of incubation in a CO2 incubator with a humidity of 5 percent.

To assess the anticancer activity through an in vitro test, the MTT assay (Mosmann, 1983) was conducted. The experiment involved plating 1 × 105 cells per well in 24-well plates, followed by incubation at 37 °C with 5% CO2. Once the cells reached confluence, various concentrations of the substances were applied and further incubated for 24 hours. After incubation, the samples were removed from the wells, washed in phosphate-buffered saline (pH 7.4) or serum-free DMEM. Subsequently, 0.5 percent 3-(4, 5-dimethyl-2-thiazolyl)-2,5-diphenyl-tetrazolium bromide (MTT) was added (100 µl/well at 5 mg/ml) and allowed to incubate for 4 hours. After the incubation period, 1 ml of DMSO was added to each well. The UV Spectrophotometer was then used to measure the absorbance at 570 nm, employing DMSO as the blank. The data obtained from these measurements were used to calculate the concentration required to inhibit 50% of the organisms (IC50). The percentage of viable cells was determined using the following formula:

% Cell viability = A570 of treated cells / A570 of control cells × 100

The X-axis of the plot represents the concentration of the sample, while the Y-axis represents the percentage of cell viability. To ensure comprehensive cell viability assessments, each assay includes both a cell control and a sample control for comparison purposes.

Table 15: Anticancer effect of Sample 3A on A431 cell line

S.No	Concentration (µg/ml)	Absorbance (O.D)			Average	Cell viability (%)
1	1000	0.185	0.187	0.183	0.185	25.91
2	500	0.229	0.228	0.228	0.228	31.93
3	250	0.273	0.275	0.271	0.273	38.23
4	125	0.318	0.317	0.319	0.318	44.53
5	62.5	0.360	0.360	0.361	0.360	50.42
6	31.2	0.402	0.404	0.400	0.402	56.30
7	15.6	0.445	0.447	0.443	0.445	62.32
8	7.8	0.484	0.482	0.486	0.484	67.78
9	Cell control	0.714				100

Figure 14: Anticancer effect of Sample 3C on A431 cell line

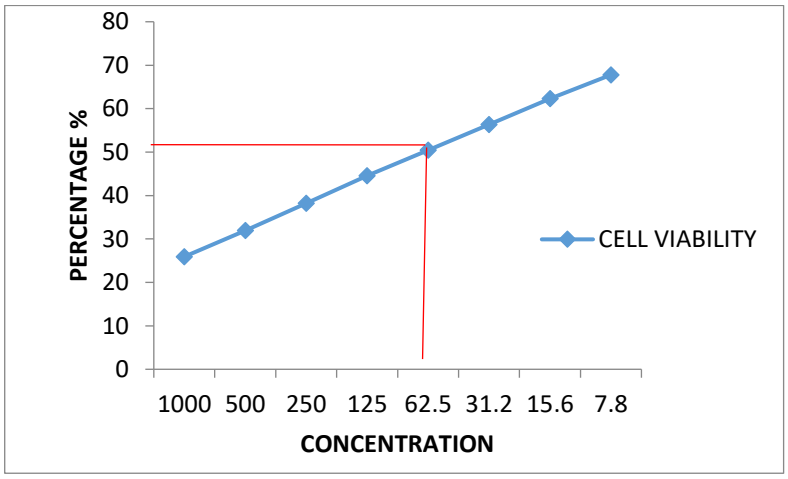

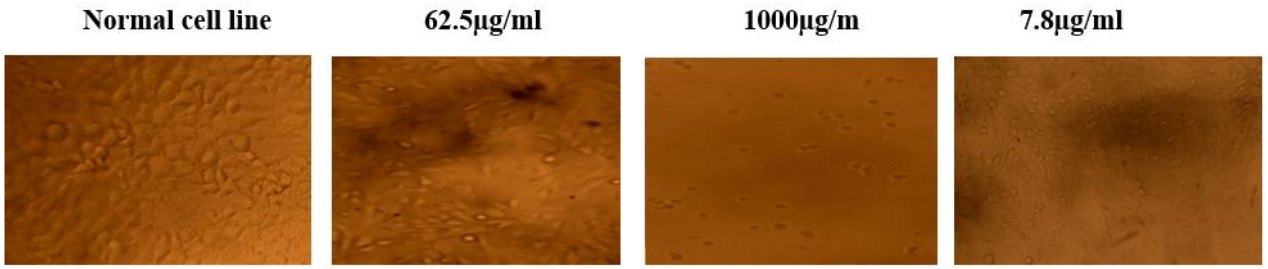

Table 16: Anticancer activity for STD using A431

S.No	Concentration (µg/ml)	Absorbance (O.D)			Average	Cell viability (%)
1	1000	0.116	0.116	0.117	0.116	16.24
2	500	0.155	0.158	0.152	0.155	21.70
3	250	0.194	0.190	0.198	0.194	27.17
4	125	0.233	0.235	0.231	0.233	32.63
5	62.5	0.272	0.274	0.270	0.272	38.09
6	31.2	0.313	0.314	0.313	0.313	43.83
7	15.6	0.351	0.352	0.351	0.351	49.15
8	7.8	0.391	0.390	0.392	0.391	54.76
9	Cell control	0.714				100

Figure 15: Anticancer effect of Standard drug on A431 cell line

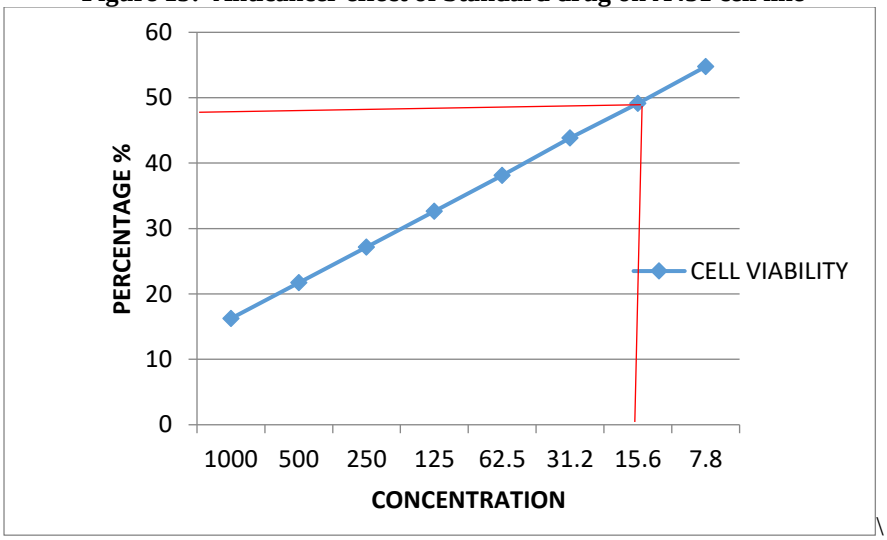

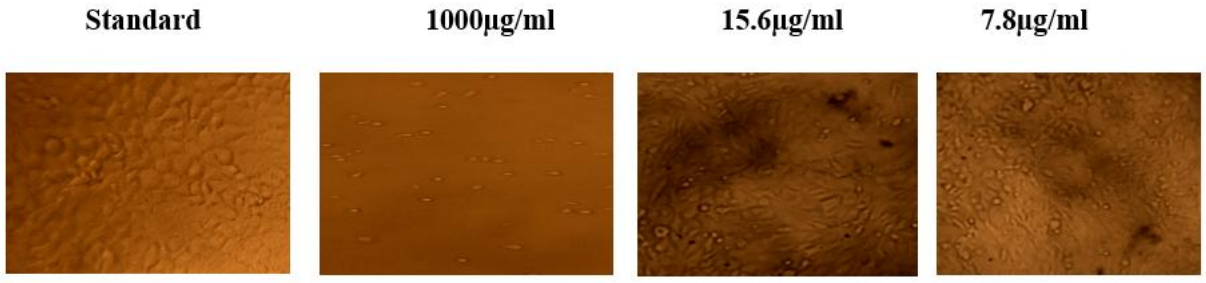

Conclusion:

The synthesised compounds were identified using 1H NMR, 13C NMR, IR, and mass spectrum analyses. The results of the investigation showed that bromooxazepine was generated. Despite these qualities, all chemicals have a variety of biological actions, including antibacterial, antifungal, anti-inflammatory, and anticancer properties. According to the data gathered, all bromooxazepine molecules have significant bioactivity. Accordingto molecular docking examinations of all ten compounds, the 3C molecule is the most active for skin cancer. Furthermore, a cell line analysis sample of the 3C molecule compared to the usual medicine demonstrated an anti-cancer influence. These pharmacological targets may also be important for drug treatments since they may lead to the development of

novel therapeutic compounds with no detrimental effects on people.

References:

1. Qadir, T., Amin, A., Sharma, P. K., Jeelani, I., & Abe, H. (2022). A review on medicinally important heterocyclic compounds. *The Open Medicinal Chemistry Journal*, *16*(1).
2. Majumdar, K. C., & Chattopadhyay, S. K. (Eds.). (2011). *Heterocycles in natural product synthesis*. John Wiley & Sons.
3. Elkanzi, N. A., Hrichi, H., Alolayan, R. A., Derafa, W., Zahou, F. M., & Bakr, R. B. (2022). Synthesis of chalcones derivatives and their biological activities: a review. *ACS omega*, *7*(32), 27769-27786.
4. Aftan, M. M., Jabbar, M. Q., Dalaf, A. H., & Salih, H. K. (2021). Application of biological activity of oxazepine and 2-azetidinone compounds and study of their liquid crystalline behavior. *Materials Today: Proceedings*, *43*, 2040-2050.
5. Rammohan, A., Reddy, J. S., Sravya, G., Rao, C. N., & Zyryanov, G. V. (2020). Chalcone synthesis, properties and medicinal applications: a review. *Environmental Chemistry Letters*, *18*, 433-458.
6. Mohammed, A. A. (2003). Briefings. *Review of African Political Economy*, *30*(97), 479-510.
7. Eftekhari-Sis, B., Zirak, M., & Akbari, A. (2013). Arylglyoxals in synthesis of heterocyclic compounds. *Chemical reviews*, *113*(5), 2958-3043.
8. Friesner, R. A., Banks, J. L., Murphy, R. B., Halgren, T. A., Klicic, J. J., Mainz, D. T., ... & Shenkin, P. S. (2004). Glide: a new approach for rapid, accurate docking and scoring. 1. Method and assessment of docking accuracy. *Journal of medicinal chemistry*, *47*(7), 1739-1749.
9. Ghose, A. K., Viswanadhan, V. N., & Wendoloski, J. J. (1999). A knowledge-based approach in designing combinatorial or medicinal chemistry libraries for drug discovery. 1. A qualitative and quantitative characterization of known drug databases. *Journal of combinatorial chemistry*, *1*(1), 55-68.
10. Glide, V. (2009). 5.5, Schrödinger. *LLC, New York, NY*.
11. Han, F. F., Li, L., Shang, B. Y., Shao, R. G., & Zhen, Y. S. (2014). Hsp90 inhibitor geldanamycin enhances the antitumor efficacy of enediyne lidamycin in association with reduced DNA damage repair. *Asian Pacific Journal of Cancer Prevention*, *15*(17), 7043-7048.
12. Kolos, N. N., Orlov, V. D., Paponov, B. V., Shishkin, O. V., Baumer, S. V., & Kvashnitskaya, N. A. (1999). Stable 1, 2, 4-triazolo [1, 5-a]-pyrimidinium salts. *Chemistry of Heterocyclic Compounds*, *35*(6), 708-715.
13. Harode, R., & Sharma, T. C. (1989). Reaction of Chalcone Dibromide with Thiourea in Presence of Potassium Hydroxide. *ChemInform*, *20*(22), no-no.
14. Singh, M. (2014). M, Kaur, O. Silakari, Flavones: an important scaffold for medicinal chemistry. *Eur. J. Med. Chem*, *84*, 206-239.
15. Saoudi, A., Hamelin, J., & Benhaoua, H. (1997). Rapid Synthesis of Aziridine Derivatives over Bentonite in "Dry Media". *ChemInform*, *28*(12), no-no.
16. El-Khawaga, A. M., Hassan, K. M., & Khalaf, A. A. (1981). Studies on Ferrocene Derivatives (VII)./Synthesis of Some New Ferrocenyl Dibromides, Benzofuranes and Indoles. *Zeitschrift für Naturforschung B*, *36*(1), 119-122.
17. Kamal, R., Kumar, R., Kumar, V., & Bhardwaj, V. (2019). Synthetic Utilization of α, β-Chalcone Dibromide In Heterocyclic Chemistry and Stereoselective Debromination. *ChemistrySelect*, *4*(39), 11578-11603.
18. Heilbron, K., Mozaffari, S. V., Vacic, V., Yue, P., Wang, W., Shi, J., ... & Wang, X. (2021). Advancing drug discovery using the power of the human genome. *The Journal of Pathology*, *254*(4), 418-429.
19. Meng, X. Y., Zhang, H. X., Mezei, M., & Cui, M. (2011). Molecular docking: a powerful approach for structure-based drug discovery. *Current computer-aided drug design*, *7*(2), 146-157.
20. Jorgensen, W. L. (2004). The many roles of computation in drug discovery. *Science*, *303*(5665), 1813-1818.
21. Bajorath, J. (2002). Integration of virtual and high-throughput screening. *Nature Reviews Drug Discovery*, *1*(11), 882-894.
22. Walters, W. P., Stahl, M. T., & Murcko, M. A. (1998). Virtual screening—an overview. *Drug discovery today*, *3*(4), 160-178.
23. Langer, T., & Hoffmann, R. D. (2001). Virtual screening an effective tool for lead structure discovery. *Current pharmaceutical design*, *7*(7), 509-527.
24. Kitchen, D. B., Decornez, H., Furr, J. R., & Bajorath, J. (2004). Docking and scoring in virtual screening for drug discovery: methods and applications. *Nature reviews Drug discovery*, *3*(11), 935-949.
25. Glide, V. (2009). 5.5, Schrödinger. *LLC, New York, NY*.
26. Han, F. F., Li, L., Shang, B. Y., Shao, R. G., & Zhen, Y. S. (2014). Hsp90 inhibitor geldanamycin enhances the antitumor efficacy of enediyne lidamycin in association with reduced DNA damage repair. *Asian Pacific Journal of Cancer Prevention*, *15*(17), 7043-7048.
27. Karplus, M., & McCammon, J. A. (2002). Molecular dynamics simulations of biomolecules. *Nature structural biology*, *9*(9), 646-652.
28. Veber, D. F., Johnson, S. R., Cheng, H. Y., Smith, B. R., Ward, K. W., & Kopple, K. D. (2002). Molecular properties that influence the oral bioavailability of drug candidates. *Journal of medicinal chemistry*, *45*(12), 2615-2623.

29. Singh, A., Vanga, S. K., Orsat, V., & Raghavan, V. (2018). Application of molecular dynamic simulation to study food proteins: A review. *Critical reviews in food science and nutrition*, *58*(16), 2779-2789.
30. Koll, T. T., Feis, S. S., Wright, M. H., Teniola, M. M., Richardson, M. M., Robles, A. I., ... & Varticovski, L. (2008). HSP90 inhibitor, DMAG, synergizes with radiation of lung cancer cells by interfering with base excision and ATM-mediated DNA repair. *Molecular cancer therapeutics*, *7*(7), 1985-1992.
31. Leo, A., Hansch, C., & Elkins, D. (1971). Partition coefficients and their uses. *Chemical reviews*, *71*(6), 525-616.
32. Brough, P. A., Aherne, W., Barril, X., Borgognoni, J., Boxall, K., Cansfield, J. E., ... & Wright, L. (2008). 4, 5-diarylisoxazole Hsp90 chaperone inhibitors: potential therapeutic agents for the treatment of cancer. *Journal of medicinal chemistry*, *51*(2), 196-218.
33. Peach, M. L., Zakharov, A. V., Liu, R., Pugliese, A., Tawa, G., Wallqvist, A., & Nicklaus, M. C. (2012). Computational tools and resources for metabolism-related property predictions. 1. Overview of publicly available (free and commercial) databases and software. *Future medicinal chemistry*, *4*(15), 1907-1932.
34. Sabitha, K., & Vijayalakshmi, R. (2012). Finding new inhibitors for EML4-ALK fusion protein: a computational approach.
35. Clark, A. J., Tiwary, P., Borrelli, K., Feng, S., Miller, E. B., Abel, R., ... & Berne, B. J. (2016). Prediction of protein–ligand binding poses via a combination of induced fit docking and metadynamics simulations. *Journal of chemical theory and computation*, *12*(6), 2990-2998.
36. Abuthakir, M. H. S., Sharmila, V., & Jeyam, M. (2021). Screening Balanites aegyptiaca for inhibitors against putative drug targets in Microsporum gypseum–Subtractive proteome, docking and simulation approach. *Infection, Genetics and Evolution*, *90*, 104755.